ELSEVIER

13 September 1996

Chemical Physics Letters 259 (1996) 488–494

CHEMICAL PHYSICS LETTERS

Coherent control by a single phase shaped femtosecond laser pulse

A. Assion, T. Baumert, J. Helbing, V. Seyfried, G. Gerber

Physikalisches Institut, Universität Würzburg, D-97074 Würzburg, Germany

Received 13 May 1996; in final form 19 June 1996

Abstract

Coherent control of molecular multiphoton ionization by a single phase shaped femtosecond laser pulse is reported. Electron and ion spectra of the sodium dimer are recorded in a molecular beam experiment and both show a strongly chirp- and pulse-length-dependent behavior. The measured spectra reveal that although for one chirp direction the population in all intermediate molecular states may be higher, the opposite chirp leads to a higher ionization yield. In addition, a strongly chirp-dependent photoionization of atomic sodium is observed.

1. Introduction

Active laser control of chemical processes has again achieved considerable interest due to progress in laser technology. For a review of this topic see, for example, Refs. [1,2]. In laboratory experiments it has been shown for small molecular systems that laser-induced processes can be directly controlled, i.e. that different product channels can be opened and closed arbitrarily by use of adequate light sources. In principle, two different control schemes are employed: within the Brumer–Shapiro scheme [3] two degenerate exit channel wavefunctions interfere constructively or destructively. This is controlled by adjusting the phase between two cw-lasers [4,5]. On the other hand in the Tannor–Kosloff–Rice scheme [6] ultrashort laser pulses are used in a pump–probe setup. A femtosecond pump laser populates an intermediate molecular state initiating wavepacket dynamics. The probe pulse is fired, when a molecular configuration is reached, which favors the desired photochemical process. Thus by simply controlling the time delay between pump and probe pulses different final products can be generated [7–9]. In order to optimize the efficiency of this control scheme different experimental approaches have been demonstrated. The amount of population on the ground and/or the excited potential energy surface can, for example, be controlled by the intensity of an ultrashort laser pulse, which coherently couples the electronic states [10,11]. Control of population in an excited state can also be obtained using the phase relation between two pulses delayed in time [12,13].

A promising way of enhancing the efficiency in this control scheme is to make use of 'tailored' femtosecond laser pulses [14–17]. The idea is to arrange the frequency components inherently belonging to an ultrashort laser pulse in a way that discriminates or enhances certain product channels. This can be achieved by amplitude and/or phase modulation of the ultrashort laser pulses. The feasibility of this approach has already been demonstrated experimen-

PII S0009-2614(96)00741-5

tally on atoms [18,19] and in pump–probe experiments on molecules [20,21].

In this letter we report the observation of the coherent control of a molecular multiphoton ionization process in a *single* pulse experiment with phase-shaped femtosecond laser pulses. The products of the laser-induced ionization process are detected by electron and ion time-of-flight spectroscopy. Kinetic energy electron spectroscopy is the ideal tool for studying the influence of phase shaped laser pulses on molecular dynamics, since the kinetic energy distribution of photoelectrons provides detailed information about the internuclear distance at which the ionization takes place [22,23]. The measured photoelectron spectra reveal that although for one chirp direction the population in all intermediate molecular states may be higher, the opposite chirp yields more of the final products. Such kind of control is desired in coherent control schemes.

2. Experiment

The experimental apparatus used to produce the ultrashort pulses applied in this experiment has been described previously in detail [9]. Femtosecond pulses at 790 nm are generated in a home-built Ti:sapphire oscillator and are amplified in a modified commercial regenerative amplifier. An optical parametric generator is used to generate 10 μJ pulses at 618 nm. The laser pulses are compressed to their transform limit of 40 fs (Gaussian) in a prism sequence (SF10 glass). The phase within the inherently spectrally broad ultrashort laser pulses is adjusted by moving one of the compressor prisms. Thus the optical pathway in the prism material and by this the amount of dispersion is controlled. The magnitude of this so called 'chirp' was determined independently by two procedures: firstly we used a micrometer screw to tune the prism position in order to record the additional optical pathway in the prism. By knowing this additional pathway the chirp could be calculated. Secondly we took intensity autocorrelations for every prism position yielding again the chirp of the laser pulses under the (verified) assumption of a Gaussian pulse shape [24]. The given magnitude of the chirp is the average of these two values regarding the deviations as error bars. In order to obtain the absolute value of the chirp the difference in material dispersion between the pathways to the autocorrelator and to the experiment was taken into account.

The experiments were performed on a cold sodium molecular beam in a differentially pumped high vacuum chamber held at a background pressure of 2×10^{-7} Torr. Na_2 was produced mainly in the lowest vibrational level of the electronic ground state by expanding pure sodium from an oven operated at 1000 K. A linear time-of-flight mass spectrometer was used for both ion and electron detection. When ionized via resonantly excited intermediate states by a ns laser, sodium atoms produce photoelectrons of well-defined energy, which served to calibrate the spectrometer. Its resolution is 50 meV for electrons of kinetic energy in the range 0.7 to 1 eV. In the actual femtosecond experiment ion and electron time-of-flight spectra were recorded under identical experimental conditions. The polarization of the femtosecond laser was parallel to the axis of the TOF spectrometer.

The 618 nm femtosecond laser beam was attenuated properly, so that the experiment could be performed at an intensity regime (below 5×10^9 W/cm^2) where perturbation theory applies for this molecule. In addition, under these experimental conditions, space charge effects are negligible. All ion and electron TOF-spectra were recorded with a 500 MHz, 2 Gigasample digital oscilloscope and averaged over several thousand laser shots.

3. Results and discussion

Fig. 1 shows a typical ion time-of-flight (TOF) spectrum taken at 618 nm with an attenuated unchirped femtosecond laser pulse. The processes leading to this spectrum are understood in detail [7,25] and sketched briefly here (Fig. 2). In all discussed multiphoton processes the Na_2 molecule is excited from $v'' = 0$ in the electronic ground state to a range of vibrational levels in the $2\,^1\Pi_g$ state resonantly enhanced by the $A\,^1\Sigma_u^+$ state. From this $2\,^1\Pi_g$ state different photoionization and fragmentation processes are possible. Process 1 is the ionization into the ionic ground state $^2\Sigma_g^+$, resulting in Na_2^+ ions and electrons having a distribution of kinetic

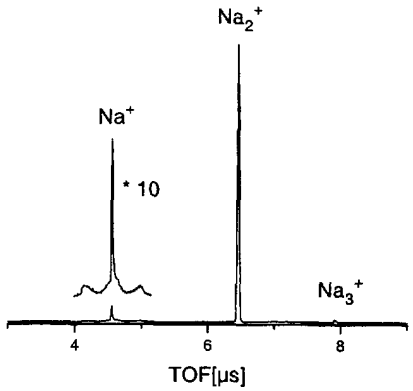

Fig. 1. Ion time-of-flight (TOF) spectrum of a sodium molecular beam taken with an attenuated unchirped femtosecond laser pulse of 40 fs duration at 618 nm. The sharp Na^+ signal arising from ionization of atomic sodium is more than one order of magnitude smaller than the Na_2^+ signal. Additionally there are fragments from the dissociation of Na_3^+ with low kinetic energy (2) and with high kinetic energy (ejected (3) in the direction and (3') opposite to the direction of the extraction field). The numbers correspond to the different processes depicted in Fig. 2.

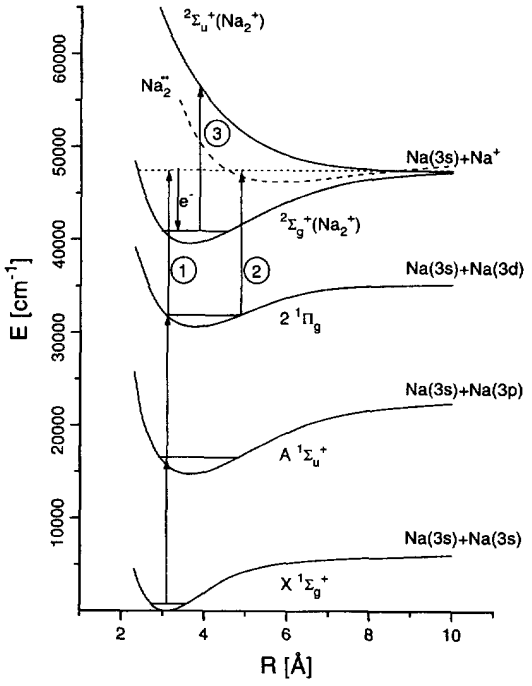

Fig. 2. Multiphoton ionization and fragmentation processes and pathways in Na_2. The Na_2 molecule is excited from $v'' = 0$ in the electronic ground state to the $2\,^1\Pi_g$ state resonantly enhanced by the $A\,^1\Sigma_u^+$ state. Three ionization and fragmentation processes 1, 2 and 3 are possible due to the absorption of further photons. For details see text.

energies from 0.7 to 1.0 eV. Process 2 is the excitation of a bound doubly excited neutral $Na_2^{**}(n,l,n',l')$ state at the outer turning point of the $2\,^1\Pi_g$ potential, followed by autoionization or autoionization induced fragmentation. Process 2 results in Na_2^+ ions and slow Na^+ fragments respectively. The corresponding electrons of less than 0.5 eV energy can be distinguished from the higher energetic electrons arising from 'direct' ionization (process 1). The fast Na^+ ions seen in the ion TOF spectrum are formed by photofragmentation (process 3) of the Na_2^+ ions produced in process 1. In addition to the kinetic ionic fragments the ion TOF spectrum also contains Na^+ ions with no initial kinetic energy. These ions are due to multiphoton ionization of the atoms contained in the sodium molecular beam.

In the present experiment we studied the dependence of the direct ionization process 1 upon the chirp of a single 618 nm femtosecond laser pulse. As all other known molecular ionization processes at 618 nm do not yield electrons in the relevant range 0.7 to 1.0 eV, energy resolved photoelectron spectroscopy allows one to investigate this process isolated from all other processes. In addition, the energy distribution of the emitted electrons provides more detailed information than ion time-of-flight spectra. Note that photoelectrons from the photoionization of atomic sodium lead only to minor substructures in the electron spectrum. This is because the Na^+ signal resulting from atomic ionization is more than one order of magnitude smaller than the Na_2^+ signal (Fig. 1). A similar argument holds in the case of the sodium trimer since no fragmentation of Na_3 was observed at the employed laser intensity. Moreover the kinetic energy of electrons arising from the sodium trimer is below 0.15 eV [26] and not relevant for our discussion.

Fig. 3a shows electron spectra measured for up-chirped (3500 ± 500 fs^2), down-chirped (-3500 ± 500 fs^2) and unchirped laser pulses. It can clearly be seen that the magnitude of the electron signal is about twice as high for up-chirped laser pulses than for down-chirped pulses. Note that the up- and down-chirped pulses are identical in all their pulse parameters, only being reversed in time. This indicates that the different ionization yields indeed are due to the phase modulation of the laser pulses and not to other effects such as different pulse durations

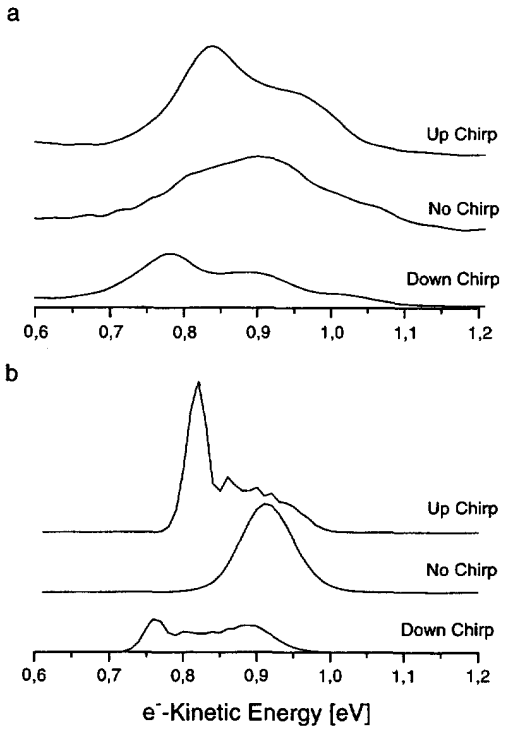

Fig. 3. (a) Measured photoelectron spectra for up-chirped (+3500 fs^2), down-chirped (−3500 fs^2) and unchirped laser pulses generated from a transform-limited 40 fs pulse at 618 nm. The duration of the chirped laser pulses is 240 fs. (b) Calculated photoelectron spectra using the same parameters as above.

or different intensity distributions. The shape of the electron spectra is also influenced by the laser chirp. However, it depends most strongly on the duration of the laser pulse, which is 40 fs for the unchirped and 240 fs for the chirped laser pulses.

In order to understand better the physical processes involved, we performed quantum mechanical calculations using the split-operator FFT method previously employed to study the interaction of 618 nm femtosecond pulses with the Na_2 molecule [27,28]. The electric field of the Gaussian laser pulse with linear chirp was used in its analytical form [24]

$$E(t) = \frac{E_0}{2\gamma^{1/4}} e^{\frac{-(t-t_n)^2}{4\beta\gamma}} e^{-i[\delta(t-t_0)^2-\varepsilon]} e^{i\omega t} + \text{c.c.},$$

where

$$\beta = \frac{\tau^2}{8\ln 2}, \quad \gamma = 1 + \frac{\phi''^2}{4\beta^2}, \quad \delta = \frac{\phi''}{8\beta^2\gamma},$$

$$\varepsilon = \tfrac{1}{2}\arctan\left(\frac{\phi''}{2\beta}\right).$$

The linear chirp is given by ϕ'', τ is the duration (FWHM) of the transform limited laser pulse($\phi'' = 0$) from which the chirped laser pulse is generated. The duration of the chirped laser pulse is then $\sqrt{\gamma}\,\tau$.

In accordance with the experimental conditions the calculations were performed in the weak field limit taking into account the relevant neutral electronic states $X\,^1\Sigma_g^+$, $A\,^1\Sigma_u^+$, and $2\,^1\Pi_g$ of Na_2. Electron spectra were calculated by coupling the $2\,^1\Pi_g$ state to the discretized continuum of the ionic ground state $Na_2^+\,^2\Sigma_g^+$. All transition dipole matrix elements were assumed to be R-independent. Additionally, the calculated electron spectra were convoluted with the resolution of the electron TOF spectrometer. The result is displayed in Fig. 3b. The calculations show qualitatively the same behavior as the measured spectra, both in the electron yield and in the energy distribution of the released electrons.

In order to understand why the ionization yield is higher for positively than for negatively chirped laser pulses we calculated the population in the $2\,^1\Pi_g$ state (the highest excited neutral state relevant in this experiment) as a function of time for both laser chirps (±3500 fs^2). The result is displayed in Fig. 4. It is clearly seen that the final population in the $2\,^1\Pi_g$ state after the end of the laser pulse is higher for down-chirped than for up-chirped pulses. This is not caused by population transfer to the ionic ground state, since in the weak field limit ionization does not significantly depopulate the $2\,^1\Pi_g$ state. The observed behavior can be understood by taking into account that the difference potential between the $2\,^1\Pi_g$ and the $A\,^1\Sigma_u^+$ state of Na_2 decreases with increasing internuclear distance. According to Mulliken's difference potential principle [29,30] the classical transition region for light induced transitions is at the internuclear distance where the difference potential equals the photon energy $\hbar\omega$. Thus for the $A\,^1\Sigma_u^+ \rightarrow 2\,^1\Pi_g$ transition, which populates the $2\,^1\Pi_g$ state, the classical transition region shifts towards larger internuclear distances for lower photon ener-

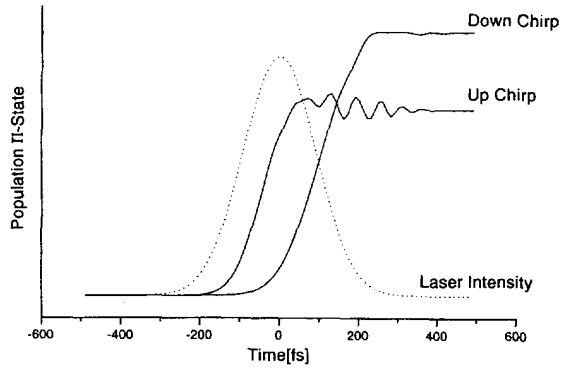

Fig. 4. Temporal development of the population in the $2\,^1\Pi_g$ state during interaction with up- and down-chirped laser pulses (± 3500 fs^2). The intensity profile of the chirped femtosecond laser is also shown. At the end of the interaction more population has been transferred to the $2\,^1\Pi_g$ state with a down-chirped laser pulse, although the excitation starts earlier when an up-chirped pulse is used.

gies and towards smaller internuclear distances for higher photon energies. This means that within the temporal course of the laser pulse this region moves inwards for up-chirped (red frequencies first) and outwards for down-chirped (blue frequencies first) laser pulses. Since the wavepacket in the $A\,^1\Sigma_u^+$ state is created at small internuclear distances and starts to propagate towards larger distances, the excitation of the $2\,^1\Pi_g$ state is more efficient for down-chirped laser pulses, because the classical transition region follows the wavepacket motion.

The question that has to be addressed now is why the ionization yield is higher for up-chirped laser pulses, although the final $2\,^1\Pi_g$ state population is higher for down-chirped laser pulses. It is the population in the $2\,^1\Pi_g$ state, which increases much earlier for the up-chirped laser pulses (Fig. 4). This temporal behavior corresponds to the fact that the Franck–Condon maxima for both the $X\,^1\Sigma_g^+ \rightarrow A\,^1\Sigma_u^+$ transition and the $A\,^1\Sigma_u^+ \rightarrow 2\,^1\Pi_g$ transition are farther to the red than the central wavelength of the femtosecond laser pulse. Thus the main part of the $A\,^1\Sigma_u^+$ and $2\,^1\Pi_g$ state's excitation takes place when the red part of the laser pulse interacts with the molecule – earlier for the up-chirped and later for the down-chirped laser pulses. For the subsequent processes, especially the direct ionization process 1, this temporal behavior is essential. In order to achieve a high ionization yield the population in the $2\,^1\Pi_g$ state must be high at maximum laser intensity. More precisely, the essential quantity is the time integral over the product of laser intensity and $2\,^1\Pi_g$ state population. This results in the interesting fact that although for a down-chirped femtosecond pulse the final population of the intermediate $2\,^1\Pi_g$ state is higher, an up-chirped pulse leads to a higher ionization yield. In other words, the up-chirped laser pulses maximize the yield of the final product Na_2^+ and minimize simultaneously the population remaining in the intermediate states. This kind of optimization is desired in coherent control schemes. Note that this effect cannot be exploited for coherent control in conventional pump–probe experiments because the probe pulse will experience the final population after the pump pulse is over.

Besides the variation of the electron yield the shape of the electron distribution can also be understood in detail. The difference potential between the ground state $^2\Sigma_g^+$ of Na_2^+ and the neutral $2\,^1\Pi_g$ state is increasing with increasing internuclear distance. Thus Mulliken's difference potential principle ($E(^2\Sigma_g^+) - E(2\,^1\Pi_g) + E(e^-) = \hbar\omega$) requires that the corresponding electron energy decreases with increasing internuclear distance. This explains why the electron energy distribution observed with unchirped laser pulse is shifted towards higher energies compared to the chirped pulse electron spectra. Because of the duration of the unchirped laser pulse (40 fs), which is much shorter than the oscillation period (~ 360 fs) of the excited vibrational levels in the $2\,^1\Pi_g$ state, the wavepacket has no time to move noticeably towards larger internuclear distances during the laser interaction. Therefore, for unchirped pulses only fast electrons are produced. The up- and down-chirped laser pulses, however, have an identical duration of about 240 fs. In this case the ionization process can take place over a wide range of internuclear distances resulting in a broad kinetic energy distribution of the photoelectrons. The apparent double structure of the electron spectra in Fig. 3 can be explained in the following way. In a time dependent picture the ionization probability per time is constant for all internuclear distances assuming an R-independent electronic dipole matrix element. However, as the wavepacket in the $2\,^1\Pi_g$ state spends

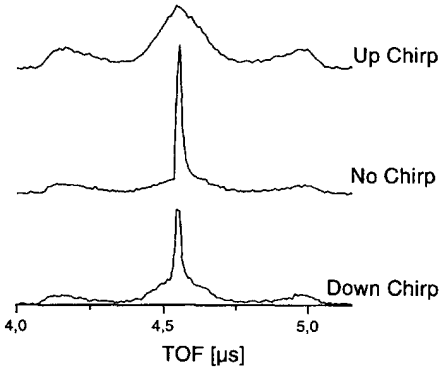

Fig. 5. Na^+ time-of-flight spectra for up-chirped ($+3500$ fs^2), down-chirped (-3500 fs^2) and unchirped laser pulses generated from a transform-limited 40 fs pulse at 618 nm. A strongly chirp dependent change of the Na^+ signal is observed.

more time at its turning points, more electrons are produced there.

In addition to the electron spectra we also measured the corresponding ion spectra depending upon the chirp of the laser pulse. Fig. 5 shows the Na^+ signal obtained for the same amount of chirp as used in the experiment displayed in Fig. 3. The most striking feature is the appearance of Na^+ ions with no initial kinetic energy for unchirped and negatively chirped femtosecond laser pulses. These ions do not originate from molecular fragmentation but from multiphoton ionization of the atoms contained in the sodium molecular beam. The atomic $3s \rightarrow 3p$ transition is induced by absorption of a photon at 589 nm from the far wing of a femtosecond laser pulse at 618 nm. Further absorption of a 616 nm photon leads to excitation of the Na(5s) state. Finally a third photon photoionizes the Na(5s) atom, producing electrons of about 1 eV kinetic energy. The different atomic multiphoton ionization efficiencies for down-chirped and up-chirped laser pulses can be understood in the following way: In a down-chirped laser pulse the frequency shifts from higher to lower frequencies within the temporal course of the pulse. Thus the 589 nm photons, which are needed in the first excitation step of the atom, are in the leading edge of the laser pulse. After the excitation of the 3p level there is still almost the full laser intensity available for subsequent photoionization. In the case of an up-chirped laser pulse, however, the Na(3p) excitation takes place when most of the laser intensity has already passed. Thus the probability for a subsequent photoionization is much lower and the Na atom remains in its 3p state. In order to prove that the laser intensity in the far wing of the pulse spectrum at 589 nm indeed is sufficient to induce the described process we used a long pass filter to suppress the 589 nm radiation. The Na^+ ions from the photoionization of parent atoms disappeared in the TOF spectra. Note that electrons arising from atomic multiphoton ionization are observed as a substructure in the electron spectra (around 1 eV) for down-chirped and unchirped laser pulses (Fig. 3a).

4. Conclusion

In a single pulse experiment using chirped femtosecond laser pulses coherent control of a molecular multiphoton ionization process was demonstrated. Both the pulse duration and the phase modulation of the ultrashort laser pulse are active control parameters. To study the influence of phase shaped laser pulses on a molecular multiphoton ionization process we employed energy-resolved electron spectroscopy. By this technique additional information is provided on the internuclear distance where the ionization process takes place. Pulse durations short compared to vibrational periods restrict the ionization process to small internuclear distances, whereas longer laser pulses lead to ionization over a wide range of internuclear distances. For identical pulse durations, however, the ionization yield for up-chirped laser pulses was about twice as high as for down-chirped pulses. Quantum mechanical calculations were performed and their results agree qualitatively with the experimental data. The calculations for the two different chirp directions show that a higher ionization yield in the multiphoton ionization process is observed, when simultaneously the population in the intermediate molecular states is minimal. This kind of optimization is desired in coherent control schemes. For atomic sodium a strongly chirp dependent resonance enhanced multiphoton ionization process was observed and related to the frequency distribution of the chirped laser pulses.

Acknowledgements

We would like to thank V. Engel for stimulating discussions and to acknowledge the experimental help of M. Strehle, B. Waibel and D. Wößner. This work has been supported by the DFG-Schwerpunktprogramm 'Femtosekunden-Spektroskopie elementarer Anregungen in Atomen, Molekülen und Clustern'.

References

[1] W.S. Warren, H. Rabitz and M. Dahleh, Science 259 (1993) 1581.
[2] M. Dahleh, A. Peirce, H. Rabitz and V. Ramakrishna, Proc. IEEE 84 (1996) 7.
[3] P. Brumer and M. Shapiro, Chem. Phys. Lett. 126 (1986) 541.
[4] V.D. Kleiman, Langchi Zhu, J. Allen and R.J. Gordon, J. Chem. Phys. 103 (1995) 10800.
[5] Ce Chen and D.S. Elliott, Phys. Rev. A 53 (1996) 272.
[6] D.J. Tannor, R. Kosloff and S.A. Rice, J. Chem. Phys. 85 (1986) 5805.
[7] T. Baumert, M. Grosser, R. Thalweiser and G. Gerber, Phys. Rev. Lett. 67 (1991) 3753.
[8] E.D. Potter, J.L. Herek, S. Pedersen, Q. Liu and A.H. Zewail, Nature 355 (1992) 66.
[9] T. Baumert and G. Gerber, Adv. At. Molec. Opt. Phys. 35 (1995) 163.
[10] T. Baumert, V. Engel, C. Meier and G. Gerber, Chem. Phys. Lett. 200 (1992) 488.
[11] T. Baumert, R. Thalweiser, V. Weiss and G. Gerber, in: Femtosecond chemistry, eds. J. Manz and L. Woeste (VCH, Weinheim, 1995) p. 397.
[12] N.F. Scherer, A.J. Ruggiero, M. Du and G.R. Fleming, J. Chem. Phys. 93 (1990) 856.
[13] V. Blanchet, M.A. Bouchene, O. Cabrol and B. Girard, Chem. Phys. Lett. 233 (1995) 491.
[14] S. Shi, A. Woody and H. Rabitz, J. Chem. Phys. 88 (1988) 6870.
[15] S. Chelkowski, A.D. Bandrauk and P.B. Corkum, Phys. Rev. Lett. 65 (1990) 2355.
[16] J.L. Krause, R.M. Whitnell, K.R. Wilson and Y.-J. Yan, in: Femtosecond chemistry, eds. J. Manz and L. Woeste (VCH, Weinheim, 1995) p. 743.
[17] M. Messina and K.R. Wilson, Chem. Phys. Lett. 241 (1995) 502.
[18] P. Balling, D.J. Maas and L.D. Noordam, Phys. Rev. A 50 (1994) 4276.
[19] J.S. Melinger, S.R. Gandhi, A. Hariharan, D. Goswami and W.S. Warren, J. Chem. Phys. 101 (1994) 6439.
[20] B. Kohler, V.V. Yakolev, J. Che, J.L. Krause, M. Messina, K.R. Wilson, N. Schwendtner, R.M. Whitnell and Y.-J. Yan, Phys. Rev. Lett. 74 (1995) 3360.
[21] C.J. Bardeen, Q. Wang and C.V. Shank, Phys. Rev. Lett. 75 (1995) 3410.
[22] C. Meier and V. Engel, Chem. Phys. Lett. 212 (1993) 691.
[23] A. Assion, J. Helbing, V. Seyfried and T. Baumert, Phys. Rev. A (1996) submitted.
[24] S. De Silvestri, P. Laporta and O. Svelto, IEEE J. Quantum Electron. 20 (1984) 533.
[25] T. Baumert, B. Buehler, R. Thalweiser and G. Gerber, Phys. Rev. Lett. 64 (1990) 733.
[26] T. Baumert, R. Thalweiser and G. Gerber, Chem. Phys. Lett. 209 (1993) 29.
[27] V. Engel, T. Baumert, C. Meier and G. Gerber, Z. Phys. D 28 (1993) 37.
[28] C. Meier and V. Engel, in: Femtosecond chemistry, eds. J. Manz and L. Woeste (VCH, Weinheim, 1995) p. 369.
[29] R.S. Mulliken, J. Chem. Phys. 55 (1971) 309.
[30] T. Baumert, B. Buehler, M. Grosser, R. Thalweiser, V. Weiss, E. Wiedenmann and G. Gerber, J. Phys. Chem. 95 (1991) 8103.